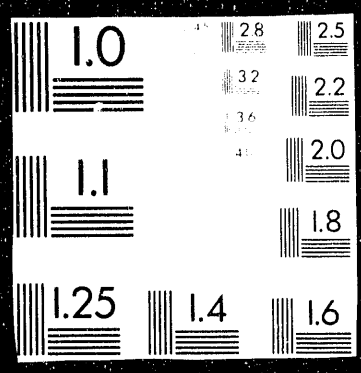

ANL/MCT/CP--77846

DE93 009965

GF-06

FORCES ON A MAGNET MOVING PAST FIGURE-EIGHT COILS

Thomas M. Mulcahy, Jialiang He*, Donald M. Rote*
Materials and Components Technology, Energy Systems* Divisions
Argonne National Laboratory, Argonne, IL. 60439

Thomas D. Rossing
Department of Physics, Northern Illinois University, De Kalb,IL. 60115

Abstract-**For the first time, the lift, drag, and guidance forces acting on a permanent magnet are measured as the magnet passes over different arrays of figure-eight (null-flux) coils. The experimental results are in good agreement with the predictions of dynamic circuit theory, which is used to explain more optimal coil arrays.**

I. INTRODUCTION

Considerable attention has been given to the magnetic levitation of vehicles over guideways consisting of periodically-spaced conducting coils. Examples of proposed guideway configurations include arrays of independent coils ("loop track") [1], interconnected coils ("ladder track") [2], two layers of coils (double-layer "null-flux" track) [3], and figure-eight coils (single-layer "null-flux" track) [4]. Typically, widely-separated superconducting magnets are mounted in the vehicle. A system that achieves both lift and guidance from vertical figure-eight coils in the guideway sidewalls has been developed in Japan [5]. This system can have a very favorable lift-to-drag ratio, if well designed.

We conducted an experimental and theoretical investigation of the lift, drag, and guidance forces on a permanent magnet moving close to various arrays of figure-eight coils. The measured time-histories of the forces provide a basis for the evaluation of electrodynamic models and codes developed to analyze the magnetic levitation of vehicles using the discrete suspension coils of the null-flux type. Good correlation was found between the experimental data and the predictions of the code COIL GDWY [6]. We report some of the results and discuss their application to the design of maglev systems.

II. EXPERIMENTAL APPARATUS

Figure-eight coils were mounted on the inside surface of a PVC drum (0.24-m inside diameter), that rotated at 1780 r/min. See Fig. 1. A 25.4-mm-square and 3.2-mm-thick NdFeB magnet was attached to a Kistler 9251A tri-axial piezoelectric force gauge and suspended over the moving coils by mounting both on a support bar. The transducer measured the three components (xyz) of the small force impulses exerted on the magnet by the induced currents and magnetic fields of the coils. The support bar was designed with high damping and resonant frequencies much greater than the force impulses' spectral frequencies. The drum was mounted on a milling-machine table that served as a reaction mass and enabled the xyz positioning of a coil. The support bar was cantilevered from a separate, massive concrete block to minimize resonant coupling between the magnet and rotating drum.

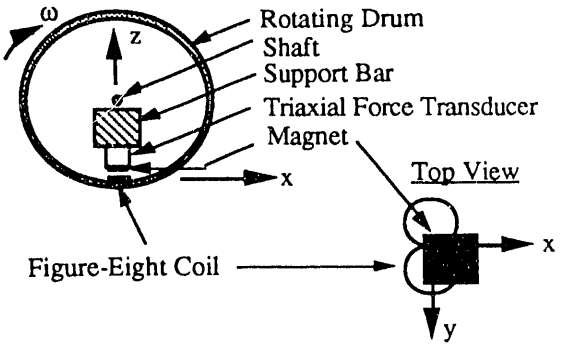

Fig. 1 Magnet mounted on force transducer over rotating coil.

A critical experimental consideration was the attachment of the magnet and the force gauge to the support bar so that cross-talk between the three sensitive axes of the force transducer was minimized, while still providing the required prestress for mounting the gauge. To calibrate the force transducers, and especially to measure cross-talk, a Bruel & Kjaer (B&K) 4810 mini-shaker was used to drive the magnet sinusoidally in each direction via a B&K 8001 impedance head with a calibrated force gauge. The frequency response of our measurement system was found to be flat (±0.5 d B) to at least 1 kHz in all three directions. The maximum cross-talk over this frequency range was found to be -20 dB (for the lift force contaminating the guidance force signal) and -25 dB or less for all other combinations.

The coils (of No. 12 copper magnet wire) were laid out sequentially around the inner surface of the drum in five configurations: Configuration A was a single coil with two 25.4-mm-square loops, as shown in Fig. 1; B was eight coils, each with two rectangular loops, 25.4 x 6.35 mm; C was four coils, each with two loops, 25.4 x 12.7 mm; D was two coils, each with two 25.4-mm-square loops; and E was four coils, each with two 25.4-mm-square loops. The areas of coil configurations B, C, and D were identical (2581 mm^2).

III. EXPERIMENTAL RESULTS

Force measurements were made for many different gaps (z) and off-center locations (y) between the magnet and the coils. The lift, drag, and guidance force waveforms acting on the

Manuscript received February 15, 1993. Work partially supported by U.S. Army Corps of Engineers: PR#E8691R001 to the U.S. Department of Energy.

DISCLAIMER

magnet are shown in Fig. 2a for y = 10.2 mm and z = 4 mm, the distance between the bottom surface of the magnet and the center plane of the coils. The y coordinate is zero when the magnet is centered over each coil (see Fig. 1), thus y = 10.2 mm means that 90% of the magnet faces one loop and 10% faces the other loop. Note that the lift force (F_y) due to a single coil (A) consists of an impulse toward the center of the coil (y = 0), followed by a slightly smaller impulse away from the center. The net force toward the center (which would serve as a lift force on a maglev vehicle) becomes more apparent in the case of two (D) and four coils (E).

The drag force (F_x) due to a single coil (A) consists of two impulses that occur when the leading and trailing edges of the magnet are centered on the coil so that the rate of change of flux through the coil is maximum. The superposition of similar pairs of impulses from 2 to 8 coils leads to waveforms B-E. In waveform E, for example, superposition of 4 pairs of impulses leads to 2 pulses of the same amplitude and 3 pulses of double amplitude in the drag force.

The guidance force (F_z) due to a single coil (A) consists of a repulsive impulse followed by a smaller attractive impulse, leading to a net force away from the coil.

IV. Theoretical Calculation of Forces and Currents

Dynamic circuit theory has been used to calculate the induced currents in the moving coils and the resultant force on the magnet. In the dynamic circuit model, an electrodynamic system is treated in terms of space- and time-dependent circuit parameters governed by a set of differential equations in matrix form. All magnetic forces existing in the system are considered as arising from changes in magnetic energy stored in the system. Currents induced in the coils and magnetic forces acting between the components of the system as a function of time or position are determined by solving the dynamic circuit equations in the time domain. Thus, the transient and dynamic performance of the system can be simulated and predicted. Previously, computer simulation models for several maglev suspension system, based on the dynamic circuit theory, have been discussed [6].

When the dynamic circuit theory is applied to our experiment, the 3.2-mm-thick permanent magnet is represented by a 25.4-mm square coil of 2260 ampere-turns. Three dimensional magnetic forces (F_x, F_y, and F_z) acting between a permanent magnet and n figure-8 coils are given, for example, as follows:

$$F_x = NI \sum_{j=i}^{n} i_j \left[\frac{\partial M_j^u}{\partial x} - \frac{\partial M_j^l}{\partial x} \right] \qquad (1)$$

where NI is the number of ampere turns of the permanent magnet, i_j is the current induced in the j^{th} figure-eight coil, and the M are the mutual inductances between the equivalent moving coil (permanent magnet) and the upper (u) and lower (l) loop of the j^{th} figure-eight coil, respectively [7]. Since the currents and mutual inductances in Eq. (1) to (3) are functions of position and time, the magnetic forces obtained from these equations are time- and space-dependent.

Waveforms for the lift, drag, and guidance forces, calculated by dynamic circuit theory, are shown in Fig. 2b. The measured waveforms (Fig. 2a) are in good agreement with those calculated. Fig. 3 shows the forces calculated at 100 m/s, for the same coil/magnet geometry investigated in Fig. 2. Although difficult to measure, the currents induced in the coils can be readily calculated by dynamic circuit theory, as shown in Fig. 4 for coil array E at 22.6 m/s.

V. Discussion of Results

The force impulses characterizing the lift and drag forces, obtained by integration of the experimental waveforms, showed that the net drag force is much larger than the net lift force. This was true for all values of y except for a narrow range between y = ±3 mm. The total lift force impulse is near zero for y = 0, increases to a maximum (about 70 μN•s for coil E at z = 5 mm) around y = 8 mm, then decreases to zero for y = 12.5 mm, and acts in the opposite direction (away from the center of the coil) for y > 12.5 mm. The drag force and guidance force reach their maximum values around y = ±12.5 mm (i.e., when the magnet passes directly opposite one of the loops of the coil. The calculations confirmed all

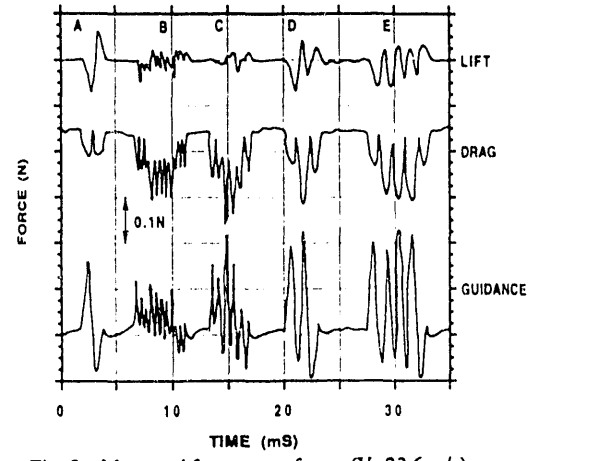

Fig. 2a. Measured force wave forms (V=22.6 m/s)

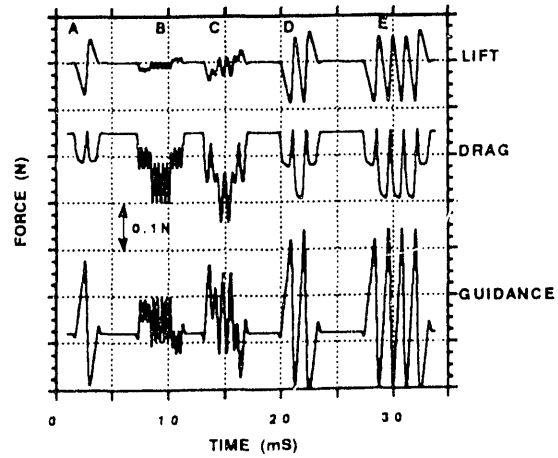

Fig. 2b Calculated force waveforms (V=22.6 m/s)

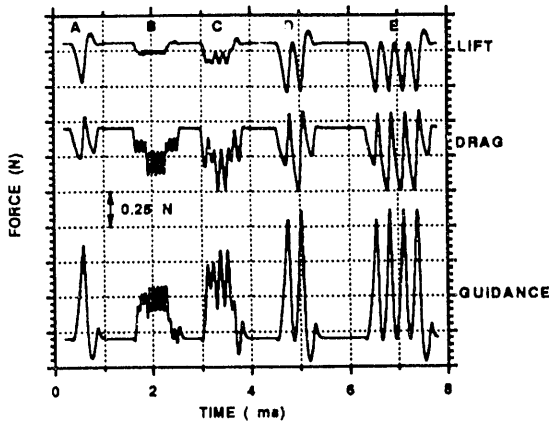

Fig. 3 Calculated force waveforms (V=100 m/s)

the above force-impulse trends.

Coils B, C, and D have the same total area. Thus it is worthwhile to compare the total lift and drag forces in order to determine their dependence on coil pitch. The following observations can be made: 1) coil D gives substantially more lift force, followed by coil C and coil B; 2) coil B gives the most drag, followed by coil C and coil D. Thus, the coil pitch should be at least as large as the magnet to obtain the best lift-to-drag ratio, for the parameter range tested.

Average lift, drag, and guidance forces, determined by integrating the calculated force-time histories and dividing by the time of passage of the magnets over a given coil, are shown in Table 1 for the conditions of Figs. 2 and 3. These results confirm the dependence of the forces on coil pitch.

As for coil array E in Fig. 4, the coil currents at 22.6 m/s were found to be essentially in phase with the position of the coils over the magnet and, therefore, with the voltages induced in the coils by the motion-dependent gradients in the magnetic field. Thus, the forces are determined mainly by the conductivity of the coil, with its inductance playing only a minor role. As the speed increases, the coil current becomes increasingly out of phase with the position. Also, the lift and guidance forces change from nearly periodic to impulsive, while the reverse occurs for drag, and the lift-to-drag ratio increases. These trends can be seen by comparing Figs. 2b and 3. As a result of the phase shift, the lift/drag and the guidance/drag force ratios increase, as indicated in Table 1 Thus, it is important to select null-flux system parameters

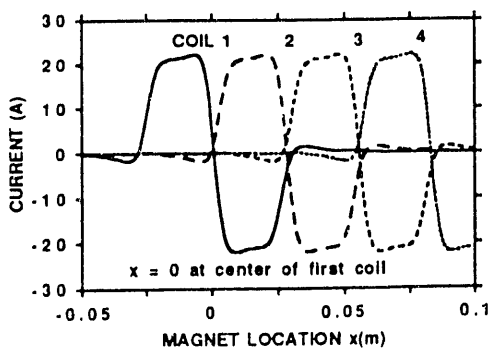

Fig. 4 Induced currents in the coils of array E for 22.6 m/s

Vel. (m/s)	Frc. (mN)	Configuration A	B	C	D	E
22.6	F_L	-11.6	-7.1	-11.1	-14.7	-14.9
100		-130	-86.6	-124	-161	-160
22.6	F_D	-90.8	-141	-159	-109	-113
100		-205	-325	-345	-238	-235
22.6	F_G	29.4	37.8	49.8	37.8	38.7
100		319	376	500	386	408
22.6	F_L/F_D	0.13	0.05	0.07	0.13	0.13
100		0.64	0.27	0.36	0.68	0.68
22.6	F_G/F_D	-0.32	-0.27	-0.44	-0.36	-0.34
100		-1.56	-1.16	-1.45	-1.62	-1.74

Table 1. Average forces and force ratios

so that the inductance dominates the resistance of the coil: the L/R time constants are large relative to the magnet's passage times (coil-width / speed).

VI. Conclusions

The good agreement between the observed and calculated impulse waveforms supports the validity of determining forces using dynamic circuit theory. Furthermore, this method provides a means for calculating coil currents, which are nearly impossible to measure.

Maximum lift occurs when the width of the figure-eight coil is nearly the same configuration as that of the magnet, and when 20% of the magnet faces one loop of the coil and 80% faces the other loop. The lift-to-drag ratio increases with speed, a decrease in the off-center position (y) of the coil, and changes in any other system parameters that increases the coil's inductive, relative to its' resistive, response.

Acknowledgements

The authors thank the other members of the AXIOM group at Argonne for many helpful discussions. In particular, they are indebted to Chris Klaus for assistance with the measurements.

References

[1] T. Ohtsuka and Y. Kyotani, "Superconducting maglev tests," *IEEE Trans. Magn.* vol. 15, pp. 1416–1421, 1979.

[2] T. Yamada, M. Iwamoto, and T. Ito, "Levitation performance of magnetically suspended high speed trains," *IEEE Trans. Magn.* vol. 8, pp. 634–635, 1972.

[3] J. R. Powell and G. T. Danby, "Magnetic suspension for levitated tracked vehicles," *Cryogenics*, vol. 11, pp. 192–204, 1971.

[4] S. Fujiwara, "Characteristics of EDS magnetic levitation having ground coils for levitation arranged on the side wall," *Trans. IEE Jpn.*, vol. 108–D, pp. 101–110,1988.

[5] S. Fujiwara and T. Fujimoto, "Characteristics of the combined levitation and guidance system using ground coils on the side wall of the guideway," *Proc. Maglev 89*, pp. 241–244, 1989.

[6] J. L. He, D. M. Rote, and H. T. Coffey, "Computation of magnetic suspension of maglev systems using dynamic circuit theory," *International Symp. Mag. Susp. Tech.*, Hampton, Virginia, August 19–23, 1991.

[7] F. W. Grover, *Impedance Calculations, Working Formulas and Tables*, New York: Dover, 1962.

END

DATE
FILMED
5/27/93